The Aeronautical Journal (2022), **126**, pp. 1853–1873
doi:10.1017/aer.2022.34

REGULAR PAPER

Accuracy of Küchemann's prediction for the locus of aerodynamic centres on swept wings compared to an inviscid panel method

B. Moorthamers* and D.F. Hunsaker

Mechanical and Aerospace Engineering, 4130 Old Main Hill, Utah State University, Logan, UT 84322-4130, USA
*Corresponding Author. Email: bmoorthamers@gmail.com

Received: 6 August 2021; **Revised:** 14 January 2022; **Accepted:** 10 March 2022

Keywords: Küchemann; aerodynamics; Analytical; Locus; Aerodynamic Center

Abstract

The locus of aerodynamic centres of a finite wing is the collection of all spanwise section aerodynamic centres, and depends on aspect ratio, wing sweep and planform shape. This locus is of great importance in the positioning of vortex elements in lifting-line theory. Traditionally, these vortex elements are placed along the quarter-chord of a wing, leading to inaccurate predictions of aerodynamic coefficients for swept wings due to the discontinuity in the line of vorticity at the wing root. An analytical solution was presented by Küchemann in 1956 to determine the locus of aerodynamic centres as a function of sweep. While experimental studies have been performed to visualise this locus, no large amount of data is available to fully evaluate the accuracy of Küchemann's analytical solution. In the present study, a numerical approach is taken using a high-order panel method for inviscid, incompressible flow to calculate the locus of aerodynamic centres for elliptic wings over a wide range of sweep angles, aspect ratios and profile thicknesses. An inviscid panel method is chosen over full CFD solutions because of their ability to isolate the inviscid phenomena. Küchemann's prediction is compared to this numerical data. The root mean square error is calculated for each wing in a broad design space to determine the accuracy of Küchemann's theory. It is shown to be remarkably accurate over the range of cases studied, with the root mean square error staying below 4% for all wings with aft sweep and aspect ratios higher than $R_A = 5$. The actual difference between Küchemann's prediction and numerical data is lower than that for the majority of the span for many of the wing designs considered, with the *RMS* error being skewed by the results at the tip. Results demonstrate that Küchemann's analytical equations can be used as an accurate approximation for the locus of aerodynamic centres and could be used in modern numerical lifting-line algorithms*.

Nomenclature

b	span
c	local chord
$\tilde{C}_L$	section lift coefficient
$\tilde{C}_{L,\alpha}$	two-dimensional lift-curve slope
$\tilde{C}_m$	section moment coefficient about the quarter-chord
$\tilde{C}_P$	section pressure coefficient
$E_{x_{ac}/c}$	difference between analytical and numerical results for chordwise aerodynamic centre position
n_s	number between 0 and 1 related to the chordwise distribution of vorticity
R_A	aspect ratio
RMS	root mean square error
x	axial coordinate

*This manuscript was previously published and presented by Moorthamers [1] at AIAA SciTech 2020 Forum in Orlando, Florida. Some statements have been slightly reworded.

© The Author(s), 2022. Published by Cambridge University Press on behalf of Royal Aeronautical Society.

https://doi.org/10.1017/aer.2022.34 Published online by Cambridge University Press

x_{ac}	axial coordinate of aerodynamic centre
y	spanwise coordinate
z	normal coordinate
y_{ac}	normal coordinate of aerodynamic centre
Δx_{ac}	deviation in chordwise aerodynamic centre position
η_{root}	spanwise distance from root as a fraction of the local chord
η_{tip}	spanwise distance from tip as a fraction of the local chord
κ_L	lift parameter used in Equation (11)
κ_m	moment parameter used in Equation (11)
λ_s	weighting function
$\Lambda_{c/2}$	half-chord sweep
$\Lambda_{c/4}$	quarter-chord sweep
Λ_e	effective sweep

1. Introduction

The numerical lifting-line algorithm of Phillips and Snyder [2] is a direct analog to the classical lifting-line theory of Prandtl [3]. It has been shown to be accurate for wings with aspect ratios greater than about 4 [2]. Similarly to Prandtl [3] in his classical lifting-line theory, the bound vortices are positioned along the wing quarter-chord line, the theoretical aerodynamic centre of a two-dimensional aerofoil according to thin aerofoil theory. The method is proven to be accurate for wings without sweep, and Phillips and Snyder [2] claim that the prediction of the lift slope for a swept wing is comparable to other potential flow and inviscid computational fluid dynamics solutions. However, the use of sweep introduces a singularity in the slope of the quarter-chord which causes strong downwash in the root region and an over-prediction of induced drag. Phillips and Snyder [2] state that in fact the locus of sections aerodynamic centres shifts aft near the root, and suggest that moving the line of vorticity to this locus would remove the discontinuity in the slope. The locus of aerofoil section aerodynamic centres is the collection of individual aerodynamic centres of spanwise sections taken from wing root to wing tip.

While the quarter-chord point is the theoretical aerodynamic centre of a two-dimensional thin aerofoil, it is not where the locus of aerodynamic centres of a finite three-dimensional wing lies. It is well known that the locus of swept wings does not follow the wing quarter-chord. Because of three-dimensional aerodynamic effects these individual section aerodynamic centres are not necessarily equal to their counterpart in two-dimensional flow. Therefore, placing the bound vortices along the quarter-chord point is a cause for error in modeling the aerodynamic properties of swept wings using lifting-line theory. It is expected that placing the vorticity instead along this locus will significantly improve the results obtained by the numerical lifting-line method proposed by Phillips and Snyder [2] for swept wings.

This research is part of a larger effort towards the research and development of morphing wings, which are of great interest to researchers in both academia and industry. The use of deforming surfaces for stability and control as opposed to traditional control surfaces is expected to decrease aerodynamic drag as well as produce a lower radar signature. The Air Force Research Lab [4–8], DARPA [9], FlexSys [10] and others [11] are developing technologies to enable such morphing surfaces. One approach that is often taken is allowing the wings to change camber at different spanwise locations along the wing. The ability to change camber over the complete wing span greatly increases the number of design variables involved with this new type of aircraft configuration. Combined with the fact that these morphing aircraft can morph mid-flight to optimise for the various flight phases they go through, these many design variables mean higher-fidelity aerodynamic analysis tools are not a viable option for use in configuration optimisation because of computational expense. This demands a computationally efficient lower-order method to rapidly explore a design space and find optimal configurations. The numerical lifting-line algorithm by Phillips and Snyder [2] provides one candidate for such a method if the aforementioned issues for swept wing calculations can be solved. Therefore, an easy way to calculate the locus of section

https://doi.org/10.1017/aer.2022.34 Published online by Cambridge University Press

aerodynamic centres needs to be found, so it could be used as an input for the placement of the bound vorticity in the numerical method.

Dietrich Küchemann [12] provides an approximation for the location of the aerodynamic centre as a function of spanwise location for a swept wing with a symmetric aerofoil of arbitrary thickness. Here we present his method of calculating the location of the locus of aerodynamic centres, but do so in a more modern notation. On a sheared wing of infinite span the line of vorticity is modeled along the same angle as the geometric sweep. In a finite wing, the interaction between vortex effects of the wing tip and wing root means the line of vorticity will never attain the angle of geometric sweep. Küchemann therefore defines the effective sweep angle to take this effect into account, and iteratively arrives at

$$\Lambda_e = \frac{\Lambda_{c/2}}{\left[1 + \left(\frac{\tilde{C}_{L,\alpha}\cos\Lambda_{c/2}}{R_A\pi}\right)^2\right]^{1/4}}, \tag{1}$$

where $\Lambda_{c/2}$ is the sweep angle of the half-chord line, $\tilde{C}_{L,\alpha}$ is the section lift-curve slope and R_A is the wing aspect ratio. In Equation (1), the local section lift curve slope $\tilde{C}_{L,\alpha}$ depends on the camber and thickness of the local aerofoil. Note that in Equation (1), Küchemann uses half-chord sweep instead of the now more conventional quarter-chord sweep. For the present work, it is assumed the quarter-chord sweep can be used directly instead of the half-chord in Equation (1). Küchemann defines a weighting function to account for the influence of wing root and tip regions dependent on the spanwise position between root and tip. The weighting function is given by

$$\lambda_s = \lambda(\eta_{\text{root}}) - \lambda(\eta_{\text{tip}}), \tag{2}$$

where

$$\lambda(\eta) = \sqrt{1 + \left(2\pi\frac{\tan\Lambda_e}{\Lambda_e}\eta\right)^2} - 2\pi\frac{\tan\Lambda_e}{\Lambda_e}\eta, \tag{3}$$

and

$$\eta_{\text{root}} \equiv \frac{y}{c}, \tag{4}$$

$$\eta_{\text{tip}} \equiv \frac{b/2 - y}{c}. \tag{5}$$

Here, b is the wing span, y is the local spanwise coordinate and c is the local chord length. In the case of wings without sweep, indeterminate terms with zero in the numerator and denominator appear in Equation (3). Therefore, L'Hospital's rule is used to evaluate Equation (3) with $\Lambda_e = 0$ as

$$\lambda(\eta)|_{\Lambda_e=0} = \sqrt{1 + (2\pi\eta)^2} - 2\pi\eta. \tag{6}$$

With the weighting function given in Equation (2) determining the amount of influence of vortex effects from the wing root and tip regions, the location of the aerodynamic centre at any spanwise location can be found from

$$\frac{x_{ac}}{c} = \frac{1 - n_s}{2}, \tag{7}$$

where

$$n_s = 1 - \frac{1 + \lambda_s\frac{\Lambda_e}{\pi/2}}{2\left[1 + \left(\frac{\tilde{C}_{L,\alpha}\cos\Lambda_e}{\pi R_A}\right)^2\right]^{\frac{1}{4(1+2|\Lambda_e|/\pi)}}}. \tag{8}$$

It should be noted that there is likely a mistake in Equation (91) in Küchemann's paper [12]. The term within parentheses of the exponent in the denominator of Equation (8) was typeset as $(1 + 2|\Lambda_e|\pi)$ in

https://doi.org/10.1017/aer.2022.34 Published online by Cambridge University Press

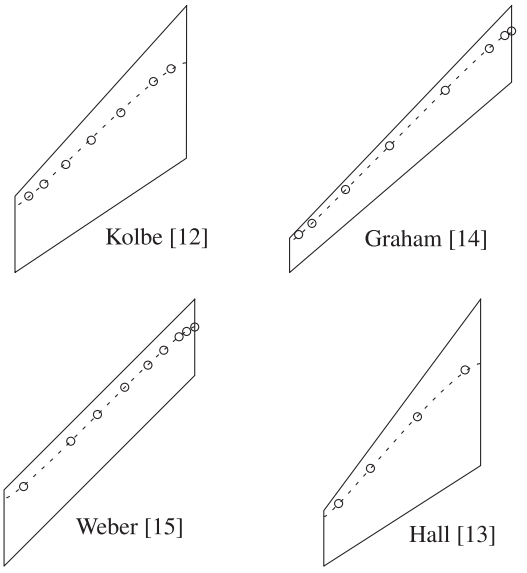

Figure 1. *Comparison of Küchemann's analytical solution [12] for the locus of section aerodynamic centres and experimental data by Kolbe [13], Hall [14], Graham [15] and Weber [16]. Data extracted from Phillips [17].*

Küchemann's paper. However, from his derivation and previous equations it can only be concluded that it has to be in fact $(1 + 2|\Lambda_e|/\pi)$, which is what is used in this study.

It is convenient to express the section aerodynamic centre location as a shift from its position in two-dimensional flow. The deviation of aerodynamic centre location relative to the two-dimensional aerodynamic centre position at any spanwise location can be calculated using Küchemann's analytical approach as

$$\left(\frac{\Delta x_{ac}}{c}\right)_{\text{Küchemann}} = \frac{1 - n_s}{2} - \left(\frac{x_{ac}}{c}\right)_{2D}. \tag{9}$$

Figure 1 shows a comparison between the locus as found using Küchemann's approach and experimental data points from others [13–16] for different wing designs. The dashed line shows the locus of section aerodynamic centres as predicted by Küchemann and the circular symbols indicate the experimental data points. The locus is seen to move forward towards the wing tip and aft towards the wing root.

While Fig. 1 shows promise for the accuracy of Küchemann's analytical approach, the amount of available experimental data for evaluation is limited. Therefore this present research uses a numerical approach using potential flow to calculate the locus of section aerodynamic centres of finite wings and generate data to evaluate the accuracy of Küchemann's work. If proven to be accurate, Küchemann's analytical approach can be suggested as an input to an ongoing research attempt to improve the existing numerical lifting-line method by Phillips and Snyder [2] for swept wings.

2. Numerical method

To evaluate the accuracy of the locus of section aerodynamic centres as calculated using Küchemann's analytical method presented in Section 1, a set of data points for swept, elliptic wings is built using an inviscid panel method. The open-source potential flow solver PANAIR is used to accurately calculate the locus of section aerodynamic centres. PANAIR is a high order panel method using linear potential flow theory for inviscid subsonic and supersonic flow simulations [18]. High Reynolds number flows approach the results of insviscid studies in the limit as the Reynolds number approaches infinity.

https://doi.org/10.1017/aer.2022.34 Published online by Cambridge University Press

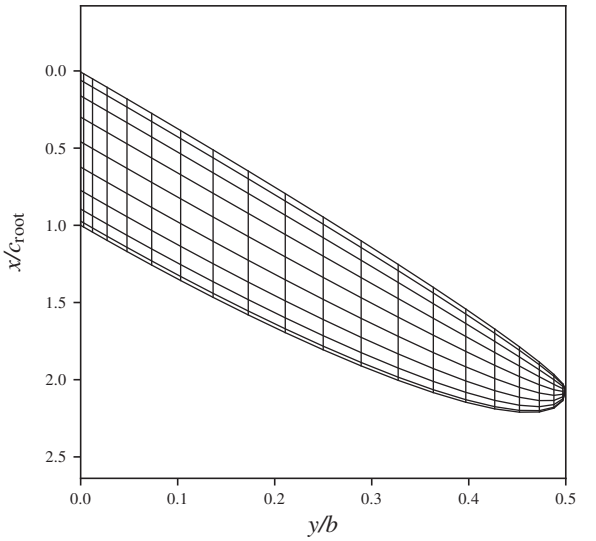

Figure 2. *Cosine-clustered grid with 20 × 20 panels. The grid used in PANAIR calculations has 80 × 80 panels.*

Other research on swept wings has been done using full CFD simulations with higher fidelity than panel codes [19, 20]. The advantage of using a potential panel code as opposed to using CFD lies in the ability to provide continuous spanwise pressure distributions thanks to the structured grid. This is harder to achieve on the unstructured grids of modern CFD codes. Because of the potential nature of the theory behind Küchemann's approximation, a panel code should be used that can fully isolate inviscid phenomena. CFD solutions will always include some viscosity. The results from PANAIR can be used to benchmark CFD solvers using the inviscid Euler equations.

Since PANAIR is well established in literature [21–23], no further validation will be provided in the scope of this research. Because PANAIR is limited by memory restrictions, a grid resolution study was performed to ensure its validity in the current research [24]. A grid consisting of 80 chordwise panels by 80 panels in the spanwise direction per semispan is used, for a total of 6400 panels per semispan. The geometry is defined using cosine-clustered quadrilateral panels with a higher concentration of nodes along the leading and trailing edges and near the wing root and tip. Only half the span of the wing needs to be meshed since PANAIR takes symmetry into account during its computations. Figure 2 shows a top-down view with a reduced number of panels for visibility purposes. The positive x-axis points towards the trailing edge of the wing, the positive y-axis is directed towards the right wing tip, and the z-axis points upward, coming out of the paper as shown in Fig. 2.

PANAIR outputs the pressure coefficient on each of the panel corner nodes as defined by

$$\tilde{C}_P = -2u_c - \left[u_c^2 + v_c^2 + w_c^2\right], \tag{10}$$

where u_c, v_c and w_c are the axial, normal and spanwise velocity components, respectively. The method detailed by Moorthamers [24] is used to integrate this pressure coefficient along each individual spanwise section of the wing in order to calculate section lift, drag, normal, axial and moment coefficients. The location of the aerodynamic centre of each spanwise section is found from

$$\frac{x_{ac}}{c} = -\frac{2\kappa_m}{\omega\kappa_L}, \tag{11}$$

$$\frac{z_{ac}}{c} = 0, \tag{12}$$

https://doi.org/10.1017/aer.2022.34 Published online by Cambridge University Press

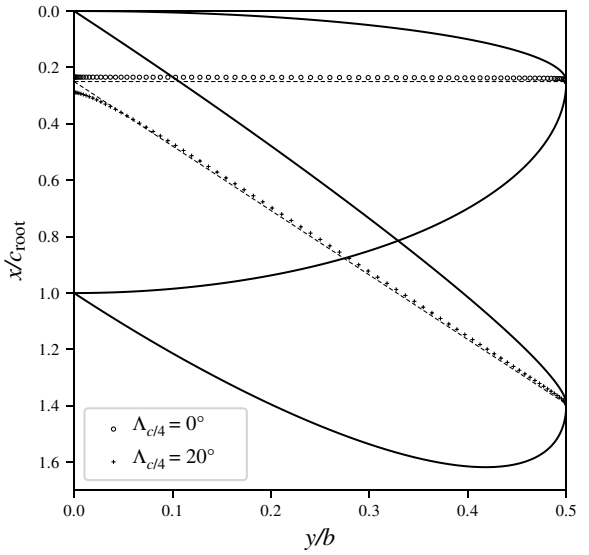

Figure 3. *Locus of section aerodynamic centres of two elliptic wings with varying quarter-chord sweep.*

where ω, κ_L and κ_m are variables used by Moorthamers [24] in the definitions of lift and moment coefficients. Equations (11) and (12) are developed from relations for the aerodynamic centre by Phillips [25] which include trigonometric and aerodynamic nonlinearities. The locus of section aerodynamic centres for a wing is then the collection of points found by applying Equations (11) and (12) at each spanwise section. It is convenient to express it as a shift with respect to the two-dimensional aerodynamic centre location, as given by Equation (13).

$$\left(\frac{\Delta x_{ac}}{c}\right)_{\text{PANAIR}} = \frac{x_{ac}}{c} - \left(\frac{x_{ac}}{c}\right)_{2D}, \tag{13}$$

where x_{ac}/c is calculated from Equation (11) and $\left(\frac{x_{ac}}{c}\right)_{2D}$ is the two-dimensional position of the aerodynamic centre for a section using the same profile.

Figure 3 shows an example of the locus as calculated from PANAIR for two elliptic wings of aspect ratio 8, one without sweep and one with a quarter-chord sweep angle of 20°.

Figure 4 shows the deviation of the locus of aerodynamic centres of the same two wings from the location of the aerodynamic centre for a two-dimensional section defined using the same profile by making use of Equation (13).

3. Results

The locus of section aerodynamic centre locations as calculated using Küchemann's analytical method given by Equation (9) is here compared to results from PANAIR. For the purpose of the present research, all wings investigated feature a NACA 0012 profile unless stated otherwise. The lift curve slope of this profile is calculated with a two-dimensional vortex panel method to be $\tilde{C}_{L,\alpha} = 6.9207$. The aerodynamic centre of a NACA 0012 aerofoil is found to lie at $(x_{ac}/c)_{2D} = 0.2619$ using the same vortex panel method. First this NACA 0012 profile will be used on a range of wing designs to understand how the accuracy of Küchemann's theory changes for varying aspect ratio and sweep angle. After this, the influence of profile thickness will be looked at and forward wing sweep is introduced to see if the conclusions still hold for this new set of wing designs.

https://doi.org/10.1017/aer.2022.34 Published online by Cambridge University Press

Table 1. *Reference wings*

	Wing I	Wing II
$\Lambda_{c/4}[^\circ]$	0	20
R_A	2	8

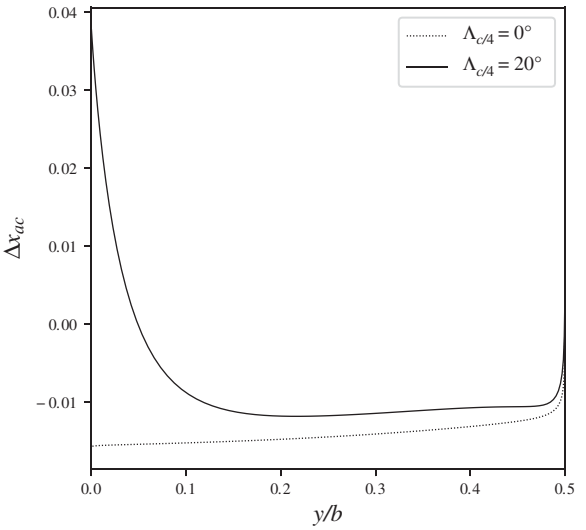

Figure 4. *Deviation Δx_{ac} as computed using PANAIR for two elliptic wings with varying quarter-chord sweep.*

3.1 Evaluation of accuracy as a function of aspect ratio and sweep

Two specific wings will be discussed before analysing the root mean square error for a large set of wings. The first is an elliptic wing with aspect ratio $R_A = 2$ and a quarter-chord sweep of $\Lambda_{c/4} = 0°$. It lies at the lower extreme of the range of design parameters included in this study and shows the largest error. The second wing is chosen as a more typical, practical wing design and features an elliptic planform with aspect ratio $R_A = 8$ and a quarter-chord sweep of $\Lambda_{c/4} = 20°$. They will be denoted as Wing I and Wing II from here onwards and are summarised in Table 1.

Figure 5 shows the locus of section aerodynamic centres for Wing I as calculated by Küchemann's analytical method and the inviscid panel method using a solid and dotted line respectively. The unswept quarter-chord line is shown as a dashed line. Note that the plot is not scaled equally on each axis for visualisation purposes.

It can be seen that for unswept, low aspect ratio wings, both the method by Küchemann and the numerical method using PANAIR predict the locus to move forward of the quarter-chord a lot over the full span of the wing. This is because of the trailing vortices originating at the wing tips are in close proximity of each other and generate downwash over the full wing. This was also hinted at by Küchemann [26] and shown to be true at the root section by Moorthamers [24]. This effect decreases as the aspect ratio increases since the influences of the tip vortices lie farther apart. Figure 6 demonstrates this using an unswept wing of aspect ratio $R_A = 30$. In this case both the analytical and numerical analyses approach the quarter-chord line as expected.

The deviation in location of each spanwise section aerodynamic centre of Wing I with respect to that of a two-dimensional NACA 0012 aerofoil in inviscid flow, located at $(x_{ac}/c)_{2D} = 0.2619$, is given in Fig. 7 using both the analytical and numerical approach. Note that the numerical solution predicts a larger shift of the aerodynamic centre than the analytic prediction. The numerical result shows a deviation of nearly 7% of the chord at the root, which is roughly 1.5% more than the analytic result. Both curves

https://doi.org/10.1017/aer.2022.34 Published online by Cambridge University Press

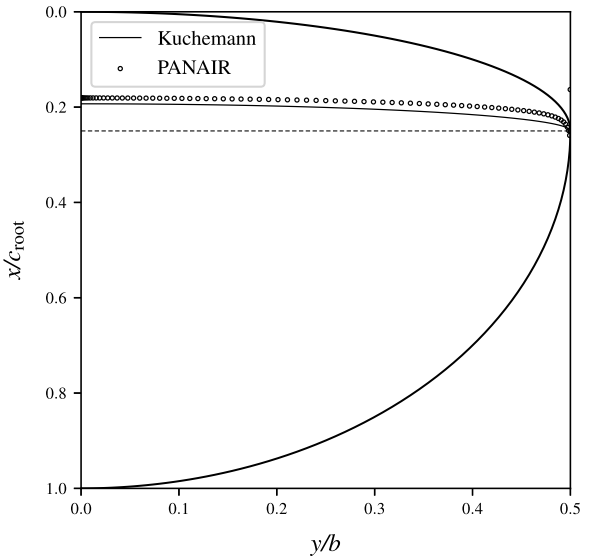

Figure 5. *Locus of section aerodynamic centres for Wing I. Quarter-chord is indicated by the dashed line.*

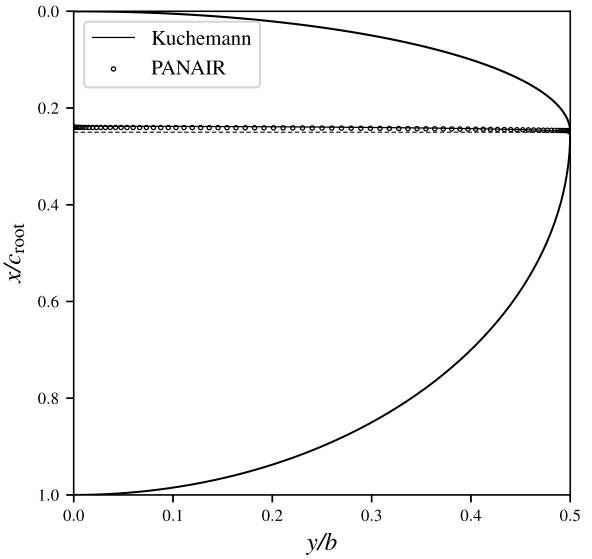

Figure 6. *Locus of section aerodynamic centres for a wing of* $R_A = 30$ *and* $\Lambda_{c/4} = 0°$. *Quarter-chord is indicated by the dashed line.*

go towards zero deviation near the tip region, meaning they approach the two-dimensional value of the section aerodynamic centre.

A similar analysis is shown for Wing II in Fig. 8. Wing II features an aspect ratio of $R_A = 8$ and a quarter-chord sweep of $\Lambda_{c/4} = 20°$. Note that again, the plot axes are not scaled equally for visualisation purposes. As predicted by theory, the locus moves aft near the wing root region because of the increased downwash produced by the bound vortices in this region and the subsequent redistribution of chordwise loading. The deviation in location of each spanwise section aerodynamic centre of this wing with respect to that of a two-dimensional NACA 0012 aerofoil in inviscid flow is given in Fig. 9. It can be seen that

https://doi.org/10.1017/aer.2022.34 Published online by Cambridge University Press

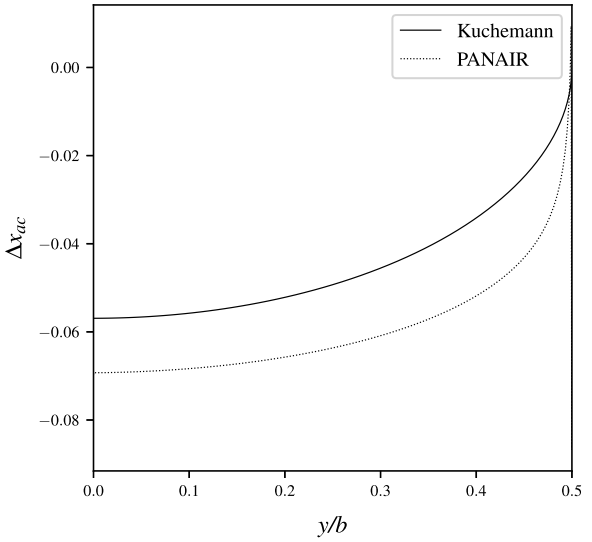

Figure 7. *Deviation Δx_{ac} from two-dimensional aerodynamic centre location for Wing I.*

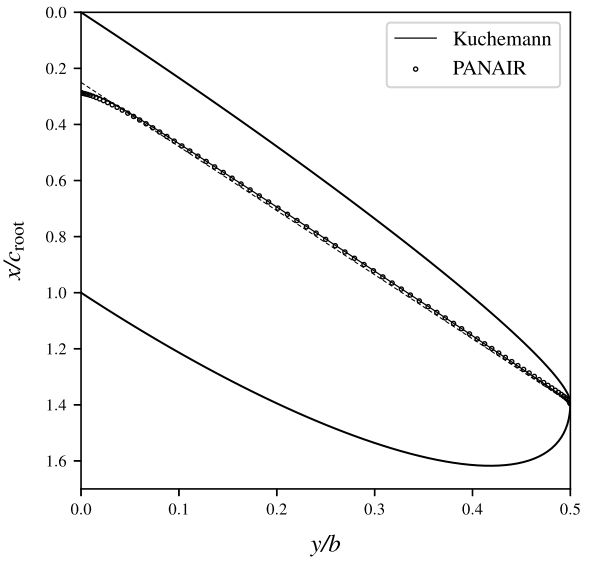

Figure 8. *Locus of section aerodynamic centres for a wing of $R_A = 8$ and $\Lambda_{c/4} = 20°$. Quarter-chord is indicated by the dashed line.*

that the curves for the analytical result and the numerical approach match more closely than was the case in Fig. 7 for the unswept wing with aspect ratio $R_A = 2$, and hence Küchemann's theory is a more accurate predictor for Wing II than for Wing I.

An evaluation of the accuracy of Küchemann's theory is made at each individual spanwise section by taking the difference of the shift in aerodynamic centre location as calculated using the numerical and analytical method as

$$E_{x_{ac}/c} = \left(\frac{\Delta x_{ac}}{c}\right)_{\text{PANAIR}} - \left(\frac{\Delta x_{ac}}{c}\right)_{\text{Küchemann}}. \tag{14}$$

https://doi.org/10.1017/aer.2022.34 Published online by Cambridge University Press

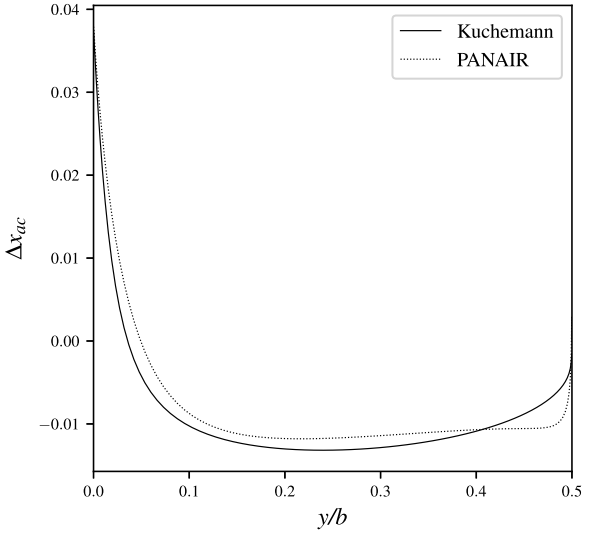

Figure 9. *Deviation Δx_{ac} from two-dimensional aerodynamic centre location for Wing II.*

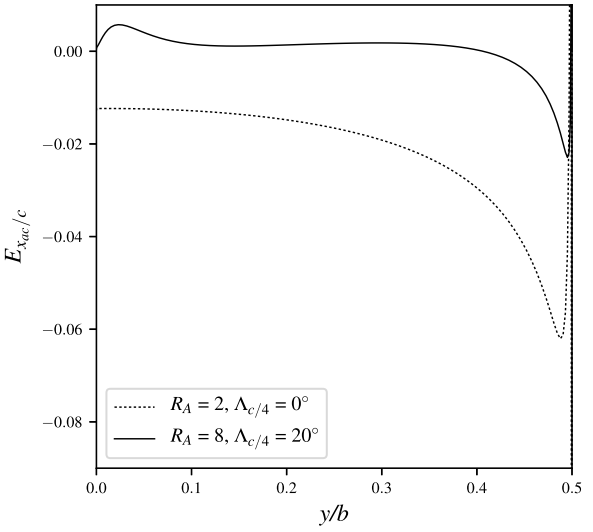

Figure 10. *$E_{x_{ac}/c}$ for Wing I and Wing II.*

The difference between the prediction by the numerical and analytical methods as defined by Equation (14), $E_{x_{ac}/c}$, is given along the span for Wing I and Wing II in Fig. 10. Note that the difference is smallest for the wing with higher aspect ratio and sweep. The sharp increase near the wing tip can be explained by considering the terms $\Delta x_{ac}/c$ in Equation (14). The presence of the chord in the denominator and the fact that this chord approaches zero for an elliptic wing means the magnitudes of the terms involved in Equation (14) increase. Also, as a consequence of the potential flow theory used in PANAIR, the sharp corners involved with the panels wrapping around the wing tip generate a sharp peak in the local lift coefficient and hence the shift of section aerodynamic centre location.

To evaluate the accuracy of Küchemann's analytic solution to the locus of aerodynamic centres over a wide range of aspect ratios and quarter-chord sweep angles, multiple numerical simulations were run to generate data for comparison. Table 2 defines limits to a range of design parameters of the swept elliptic wings for which the locus of aerodynamic centres is investigated.

https://doi.org/10.1017/aer.2022.34 Published online by Cambridge University Press

Table 2. *Range of design parameters*

Design parameter	Value	Step size
$\Lambda_{c/4}[^\circ]$	$0 - +40$	1
R_A	$2 - 30$	1
Aerofoil	NACA 0012	

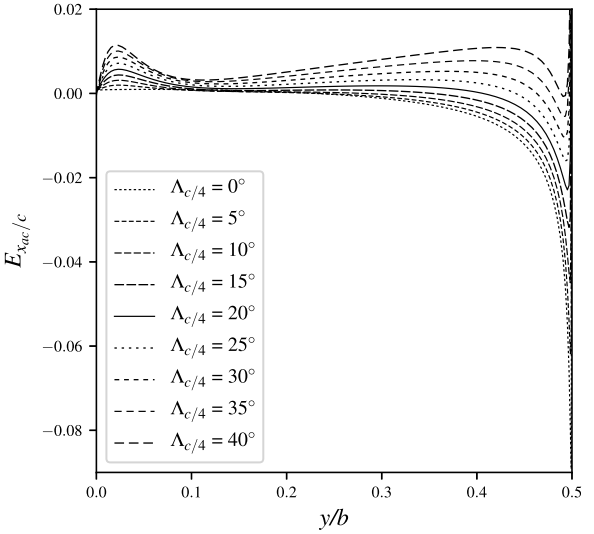

Figure 11. *$E_{x_{ac}/c}$ for wings of $R_A = 8$ and different quarter-chord sweep angles.*

Figure 11 shows $E_{x_{ac}/c}$ along the complete wing semispan for varying quarter-chord sweep angles with constant aspect ratio. Wing II is depicted using a solid line as a reference. It can be seen that as the wing sweep increases and hence the locus moves away from the two-dimensional aerodynamic centre, the difference between the numerical and analytical result increases over the whole span. It stays within 1% of the local chord for 90% of the semispan for all sweep angles, only increasing beyond that at the tip, where the small chord amplifies the differences. Note that at high enough sweep angles, $E_{x_{ac}/c}$ turns positive as opposed to low sweep angles. This means that Küchemann predicts a farther shift aft than the numerical approach at low sweep angles whereas at higher sweep angles the numerical prediction will lie aft of the analytical result.

To see the effect of aspect ratio on the accuracy of Küchemann's theory according to Equation (14), Fig. 12 shows $E_{x_{ac}/c}$ for wings with a quarter-chord sweep angle $\Lambda_{c/4} = 20^\circ$ and different aspect ratios. Again Wing II is the solid reference line. Note that the accuracy greatly decreases with decreasing aspect ratio, but still lies within 2.5% of the local chord length of the numerical result for the lowest aspect ratio. It can be seen that Küchemann's theory becomes more accurate with increasing aspect ratio.

Figure 13 shows how far the local aerodynamic centre at the root section shifts from the two-dimensional aerodynamic centre location for aft swept wings of varying sweep and aspect ratio using a NACA 0012 profile. The curves show the prediction using Küchemann's approach as a function of aspect ratio with different lines for different sweep angles, while the dots indicate the numerical results using PANAIR. It shows that for increasing wing sweep the local section aerodynamic centre moves aft. For increasing aspect ratio, the local section aerodynamic centre moves aft until it reaches a nearly constant shift, with $(\Delta x_{ac}/c)_{root}$ not increasing with aspect ratio beyond roughly $R_A = 12$. It can be seen that the analytical and numerical prediction of the shift at the root section line up very well for aft swept wings.

https://doi.org/10.1017/aer.2022.34 Published online by Cambridge University Press

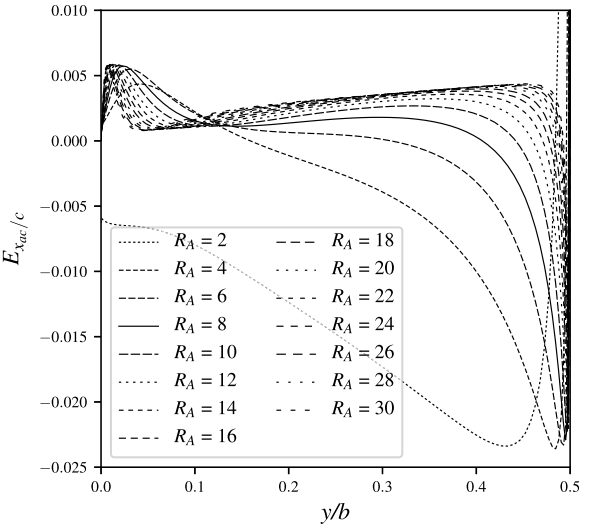

Figure 12. *$E_{x_{ac}/c}$ for wings with $\Lambda_{c/4} = 20°$ and different aspect ratios.*

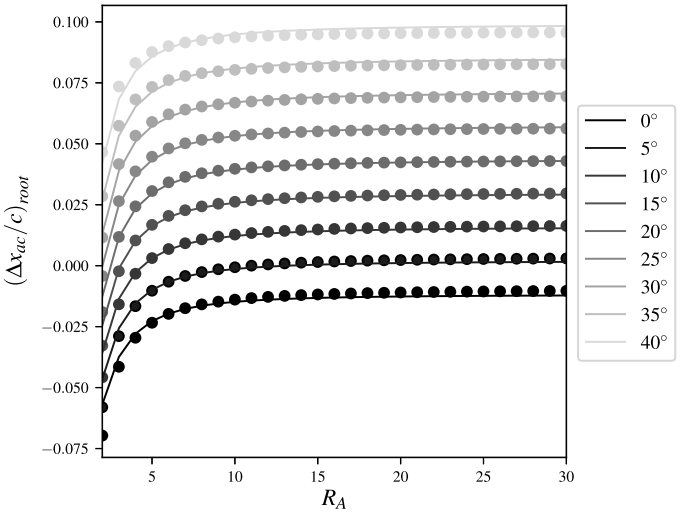

Figure 13. *$\Delta x_{ac}/c$ at centre section for elliptic wings of varying aspect ratio and sweep angles.*

For an overview of how accurate Küchemann's approach is for the full set of wing designs as defined in Table 2, the root mean square error is defined as:

$$RMS = \sqrt{\frac{1}{n}\left(\left(E_{x_{ac}/c}\right)_1^2 + \left(E_{x_{ac}/c}\right)_2^2 + \ldots \left(E_{x_{ac}/c}\right)_n^2\right)}. \tag{15}$$

Here, $\left(E_{x_{ac}/c}\right)_n$ is the difference between the section aerodynamic centre location as predicted by PANAIR and Küchemann as defined in Equation (14). It is calculated at each spanwise location with a total of $n = 80$ locations along the semispan. Because of the node clustering near the wing root and the wing tip, the difference $E_{x_{ac}/c}$ in these regions carries a more significant weight in the *RMS* calculation than the differences along the mid-portion of the span. Figure 14 shows the root mean square error as a function of aspect ratio for lines of constant sweep angle on a logarithmic vertical axis.

https://doi.org/10.1017/aer.2022.34 Published online by Cambridge University Press

Table 3. *Aerofoil data*

Aerofoil	$\tilde{C}_{L,\alpha}$	$(x_{ac}/c)_{2D}$
NACA 0012	6.9207	0.2619
NACA 0015	7.0885	0.2657
NACA 0018	7.2515	0.2696
NACA 0021	7.4152	0.2738

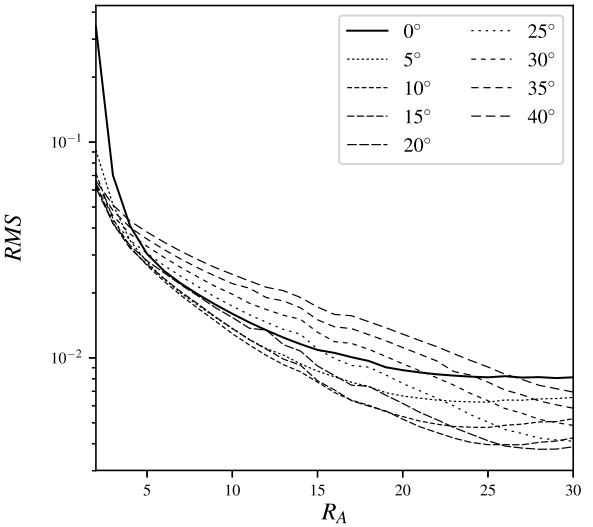

Figure 14. *Root mean square error of $E_{x_{ac}/c}$ for all wings defined in Table 1.*

From Fig. 14 one can deduce that for all wings with aft sweep and aspect ratios higher than $R_A = 5$, the *RMS* is below 4% of the local chord. Küchemann's theory for an estimation of the locus of section aerodynamic centres therefore seems accurate when compared to numerical data using PANAIR. Comparing the line for a quarter-chord sweep angle of $\Lambda_{c/4} = 20°$ in Fig. 14 to the values for $E_{x_{ac}/c}$ in Fig. 12 shows that the *RMS* is skewed by the large differences in the cosine-clustered tip regions, but the actual difference $E_{x_{ac}/c}$ is much lower than the *RMS* would indicate over most of the span.

3.2 Evaluation of accuracy with thickness variation

Figure 14 shows that Küchemann's analytic derivation offers a reasonable approach to calculating the locus of section aerodynamic centres for swept elliptic wings featuring a NACA 0012 profile with an aspect ratio between 2 and 30 and a quarter-chord sweep angle between 0° and 40°. To see whether this theoretical approach is valid over a wider range of wing designs, wings with a thickness-to-chord ratio of between 12% and 21% are investigated. Table 2 describes the aerofoils used in the investigation, their respective lift curve slopes $\tilde{C}_{L,\alpha}$ and the location of their aerodynamic centre for a profile in two-dimensional flow $(x_{ac}/c)_{2D}$ as calculated using a vortex panel method.

Figures 15 and 16 show $E_{x_{ac}/c}$ for Wing I and Wing II respectively using all thicknesses mentioned in Table 3.

In the case of Wing I, the magnitude of $E_{x_{ac}/c}$ is seen to increase for increasing wing thickness whereas for Wing II, the magnitude is lower for thicker aerofoil profiles over the majority of the wing span. However, Fig. 17 shows that the root mean square error does not necessarily reflect this over a wide range of wings with geometry defined by Table 1 and thicknesses defined by Table 2. Isolating the

https://doi.org/10.1017/aer.2022.34 Published online by Cambridge University Press

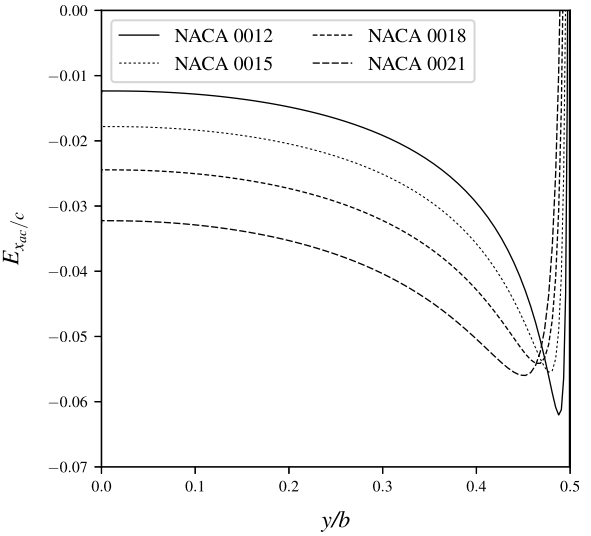

Figure 15. *$E_{x_{ac}/c}$ for Wing I with varying profile thickness.*

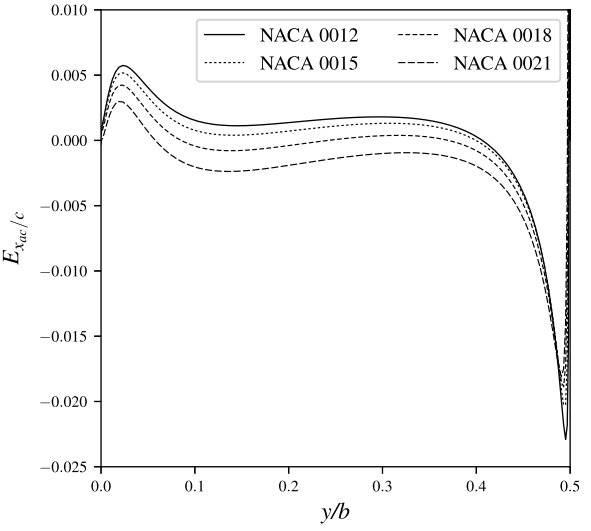

Figure 16. *$E_{x_{ac}/c}$ for Wing II with varying profile thickness.*

lines for wings with quarter-chord sweep $\Lambda_{c/4} = 20°$ in Fig. 18, the *RMS* is actually seen to increase for increasing aerofoil thickness over all aspect ratios tested.

To understand why this happens, Figs 19 and 20 show a zoomed-in view of the locus of section aerodynamic centres as calculated by Küchemann's theory and by the numerical method for a wing of $R_A = 8$ and $\Lambda_{c/4} = 20°$ for all thicknesses defined in Table 3. The differences between Küchemann and PANAIR at the tip are larger for thicker aerofoils. Since the chord is small and hence $E_{x_{ac}/c}$ is large at the tip, this greatly magnifies the *RMS*. However, it should be noted that over the majority of the span, the numerical and analytical results match very closely.

Despite the slight increase in *RMS* with increasing thickness, Fig. 17 shows that it is still below 4% for all wings with aspect ratios higher than $R_A = 5$, and therefore Küchemann's analytic approach gives a reasonable estimation for the locus of section aerodynamic centres.

https://doi.org/10.1017/aer.2022.34 Published online by Cambridge University Press

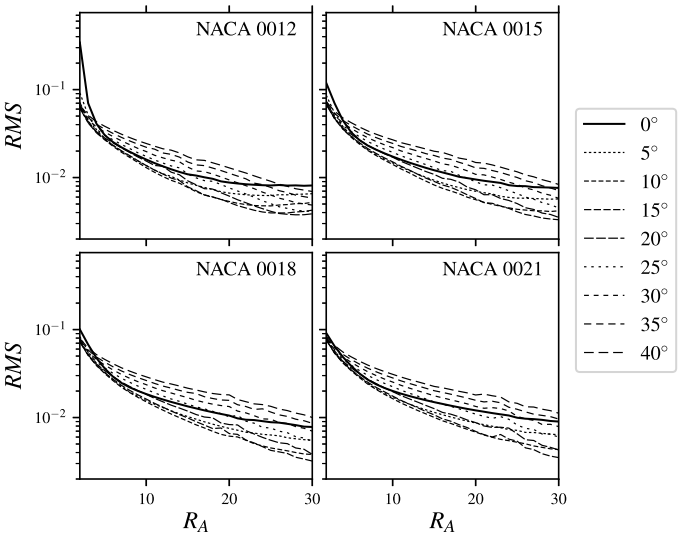

Figure 17. *Root mean square error of $E_{x_{ac}/c}$ for all wings defined in Table 1 for different profile thickness.*

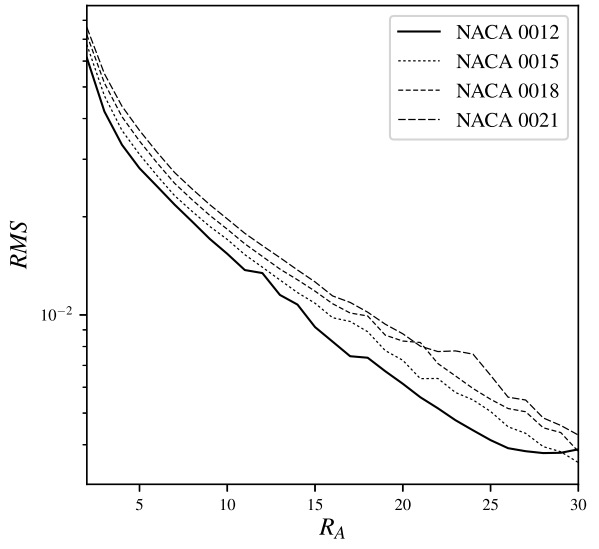

Figure 18. *Root mean square error of $E_{x_{ac}/c}$ for wings with a sweep angle of $\Lambda_{c/4} = 20°$ and varying aspect ratio with different lines for different profile thickness.*

3.3 Evaluation of accuracy for forward-swept wings

This section discusses the accuracy of Küchemann's analytic derivation for the locus of section aerodynamic centres for forward-swept wings. Wings with forward sweep can be of interest to aircraft designers because of their favourable properties at high angles of attack. Their inboard sections will stall first, allowing aileron control authority at high angles of attack. They are also suggested to be beneficial for use in wing designs with natural laminar flow. With the advent of composite structures, forward-swept wings are more feasible to produce and hence might see an increased use in aircraft design [27].

Figure 21 shows an elliptic wing of aspect ratio $R_A = 8$ and a quarter-chord sweep angle of $\Lambda_{c/4} = -20°$ and its locus of section aerodynamic centres as calculated by Küchemann's theory as well as

https://doi.org/10.1017/aer.2022.34 Published online by Cambridge University Press

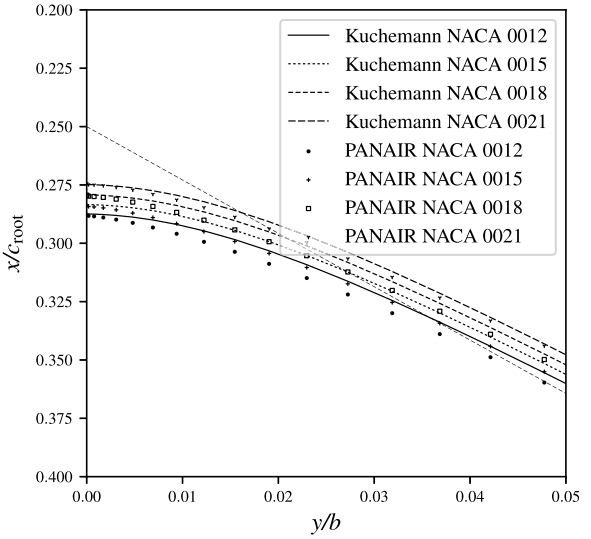

Figure 19. *Magnified view of the locus of section aerodynamic centres near the centre region for Wing I with varying profile thickness. Quarter-chord is indicated by the dashed line.*

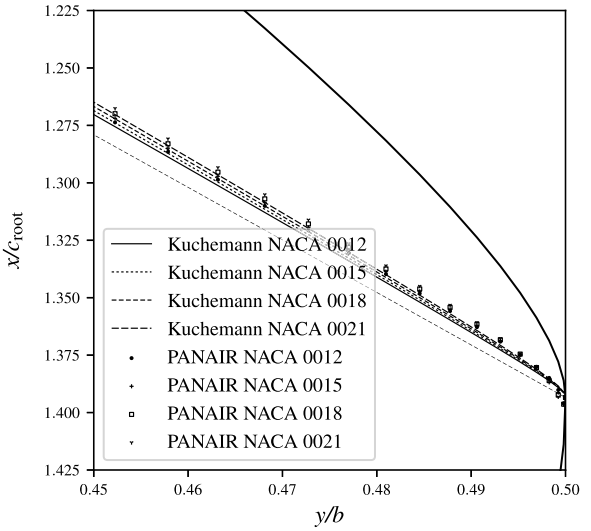

Figure 20. *Magnified view of the locus of section aerodynamic centres near the tip region for Wing II with varying profile thickness. Quarter-chord is indicated by the dashed line.*

calculated using the numerical panel method. The locus moves forward near the wing root, opposite to the behaviour present in a wing swept backwards.

Figures 22 and 23 show a zoomed view of the root region and tip region, respectively, for all wing thicknesses in Table 3. It can be seen that the numerical and analytical approach match well in the root region, with the difference between numerical and analytical result increasing for increasing thickness. However, while Küchemann predicts the locus to follow the quarter chord closely out towards the tip, the numerical approach using PANAIR shows it to move forward in the outer regions of the wing.

The behaviour at the tip shown in Fig. 23 suggests a bad prediction of the locus by Küchemann as compared to the numerical calculation and a high negative value for $E_{x_{ac}/c}$, as is confirmed in Fig. 24 for

https://doi.org/10.1017/aer.2022.34 Published online by Cambridge University Press

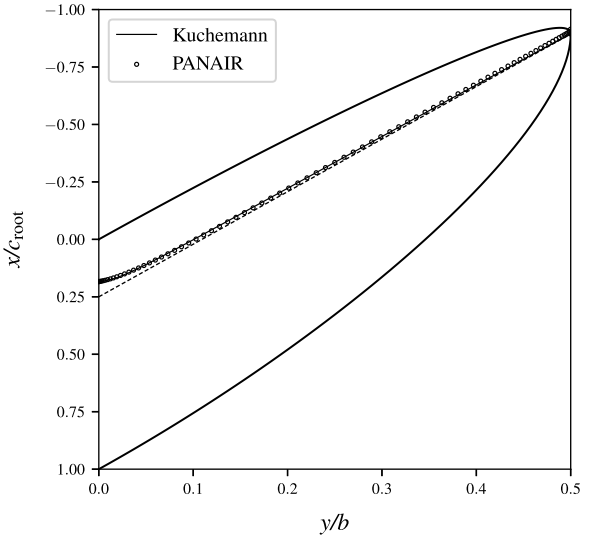

Figure 21. *Locus of section aerodynamic centres for a wing of $R_A = 8$ and $\Lambda_{c/4} = -20°$. Quarter-chord is indicated by the dashed line.*

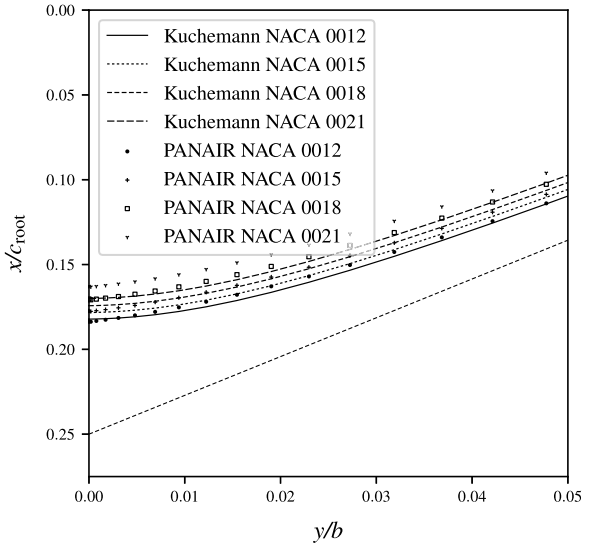

Figure 22. *Magnified view of the locus of section aerodynamic centres near the centre region for a wing of $R_A = 8$ and $\Lambda_{c/4} = -20°$ and varying profile thickness. Quarter-chord is indicated by the dashed line.*

all profile thicknesses defined in Table 3. Note that the lower limit on the vertical axis was chosen for plotting purposes, but that the difference $E_{x_{ac}/c}$ does in fact exceed 25% of the local chord length.

On first inspection, with the exception of the very outboard portion of the wing, Fig. 24 suggests that Küchemann's analytic derivation correctly predicts the locus of section aerodynamic centres over the majority of the span of this particular elliptic wing of aspect ratio $R_A = 8$ and a quarter-chord sweep angle of $\Lambda_{c/4} = -20°$. To judge the accuracy of the theory over a wide range of forward-swept wing designs, the root mean square error as defined by Equation (15) is calculated for the wings defined in Table 4. The aerodynamic data from Table 3 was used. The results for the *RMS* across the whole design space of forward-swept wings are shown in Fig. 25.

https://doi.org/10.1017/aer.2022.34 Published online by Cambridge University Press

Table 4. *Range of design parameters for forward-swept wings*

Design Parameter	Value	Step Size
$\Lambda_{c/4}[^\circ]$	$0 - -40$	-1
R_A	$2 - 30$	1
Aerofoil	NACA 0012 – 0021	3%

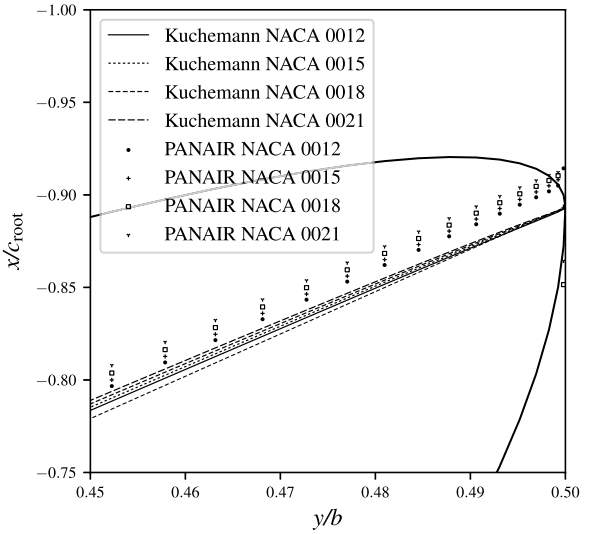

Figure 23. *Magnified view of the locus of section aerodynamic centres near the tip region for a wing of $R_A = 8$ and $\Lambda_{c/4} = -20^\circ$ and varying profile thickness. Quarter-chord is indicated by the dashed line.*

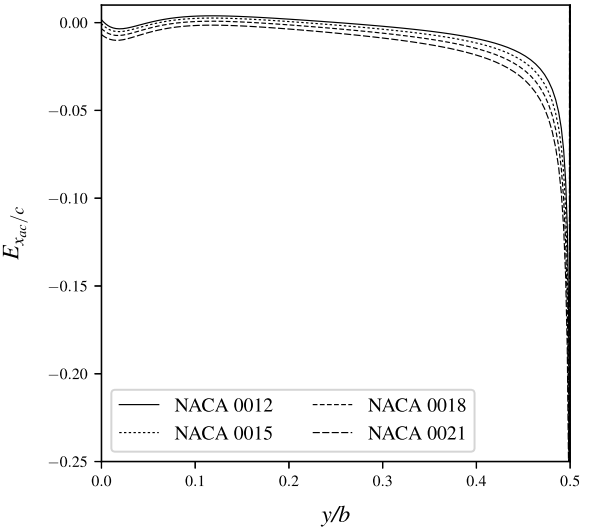

Figure 24. *$E_{x_{ac}/c}$ for a wing with $R_A = 8$, $\Lambda_{c/4} = -20^\circ$ and varying profile thickness.*

https://doi.org/10.1017/aer.2022.34 Published online by Cambridge University Press

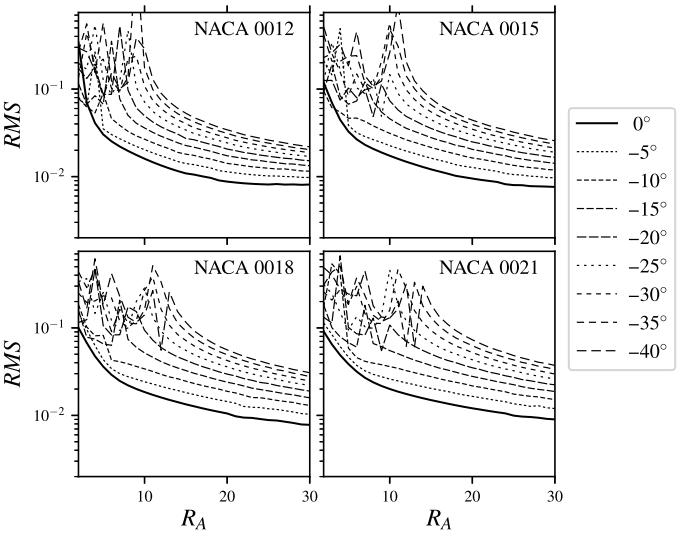

Figure 25. *Root mean square error of $E_{x_{ac}/c}$ for all wings defined in Table 3.*

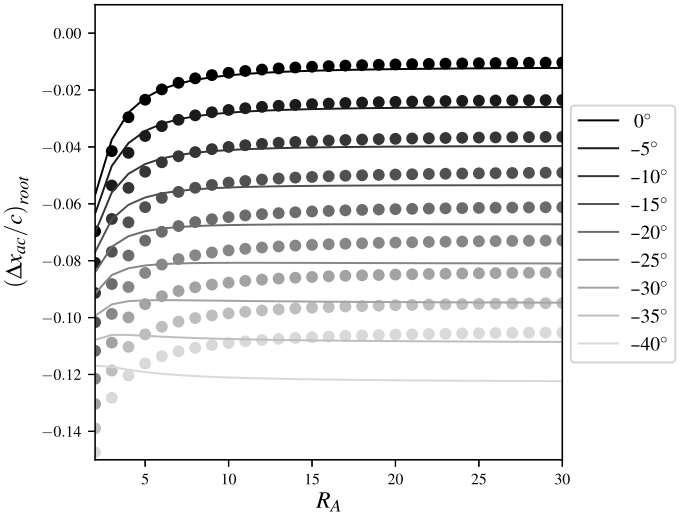

Figure 26. *$\Delta x_{ac}/c$ at centre section for elliptic wings of varying aspect ratio and sweep angles.*

Comparing Fig. 25 and Fig. 17 and using the zero-sweep curve as a reference shows that overall, the *RMS* is higher for the forward-swept wings than for the wings with a positive sweep angle. This is due to the incorrect prediction of the moving forward of the locus in the outboard portion of the wing as pointed out in the discussion of Fig. 23. A similar trend to the rearward swept wings can be seen where the *RMS* slightly decreases for increasing thickness at low or zero sweep, but the spread of the curves for increasing sweep increases with increasing thickness. The peaks present at low aspect ratios are due to some specific aspect ratio and sweep combinations that cause numerically erratic behaviour within PANAIR.

Figure 26 shows the deviation of the aerodynamic centre from its two-dimensional position as calculated by both the analytical and numerical approach at the root section of wings using a NACA 0012 profile as a function of aspect ratio for varying forward sweep angles. Figure 22 shows that for that particular wing with aspect ratio $R_A = 8$ and quarter-chord sweep angle of $\Lambda_{c/4} = -20°$, Küchemann and

https://doi.org/10.1017/aer.2022.34 Published online by Cambridge University Press

PANAIR agree well. However, Fig. 26 shows that at low aspect ratios and high sweep combinations, Küchemann fails to correctly predict the forward shift of the locus by up to 2.5% of the local chord difference.

From Fig. 25 we can tell that the *RMS* reaches values higher than 10% for some forward-swept wing designs. However, the *RMS* is mainly driven by the behaviour out towards the wing tips, where the difference between analytical and numerical results are largest. Still, for forward-swept wings, extra care has to be taken when using Küchemann's analytic derivation as a prediction of the locus of section aerodynamic centres.

4. Conclusions

An evaluation of Küchemann's analytic solution for the locus of section aerodynamic centres is made by comparing it to a numerical data set. His method is outlined and summarised using modern notation in Equations (1)–(9). The numerical approach uses the inviscid, incompressible panel method PANAIR to generate data for the wide range of finite, swept, elliptic wings specified by Tables 2 and 4 for different thicknesses specified in Table 3. Figure 10 shows that Küchemann's solution becomes increasingly accurate for wings of higher aspect ratio, with the difference in numerical and analytical result $E_{x_{ac}/c}$ demonstrated for two example wings and the highest difference being recorded for a wing of aspect ratio $R_A = 2$ and a quarter-chord sweep of $\Lambda_{c/4} = 0°$. For this wing using a NACA 0012 profile, the difference remains within 1.5% of the local chord near the wing root but grows to roughly 6% of the local chord near the wing tip.

The wing design of aspect ratio $R_A = 8$ and a quarter-chord sweep of $\Lambda_{c/4} = 20°$ is subjected to a sensitivity study of varying sweep or aspect ratio in Figs 11 and 12 respectively. For the full range of wing designs with aft sweep and featuring a NACA 0012 profile, Fig. 14 shows that the root mean square error stays within 4% for wings with aft sweep and aspect ratios higher than $R_A = 5$. The actual difference between Küchemann's analytic solution and the numerical data as calculated using PANAIR is lower than this number for the majority of the span. This is true for all profile thicknesses as shown in Fig. 17.

In forward-swept wing designs, Fig. 23 shows a noticeable difference between Küchemann and the numerical solver result on the outboard wing sections. This makes the *RMS* go over 10% for select wing designs as seen in Fig. 25. Therefore, more care must be taken when using Küchemann's analytical solution to determine the locus on forward swept wings.

In summary, we can conclude that Küchemann has derived an accurate method for prediction of the locus of section aerodynamic centres as compared to a high order panel method. For conceptual design stages where multiple wings need analysing in a short time frame, it is recommended to be used. Forward-swept wings show a higher discrepancy between Küchemann's analytical method and the numerical approach. Once the design reaches a more mature state, it is recommended to use a higher order method at the cost of a larger computational expense.

Acknowledgments. This work was funded by the U.S. Office of Naval Research Sea-Based Aviation program (Grant No. N00014-18-1-2502) with Brian Holm-Hansen as the program officer.

References

1. Moorthamers, B. and Hunsaker, D.F. "Accuracy of Küchemann's prediction for the locus of aerodynamic centres on swept wings," *AIAA SciTech 2020 Forum*, Orlando, Florida, 2020.
2. Phillips, W. and Snyder, D. "Modern adaptation of Prandtl's classic lifting-line theory," *J Aircr*, 2000, **37**, (4), pp 662–670.
3. Prandtl, L. "Tragflügel Theorie," Nachrichten von der Gesellschaft der Wisseschaften zu Göttingen, 1918, pp 451–477.
4. Marks, C.R., Zientarski, L., Culler, A.J., Hagen, B., Smyers, B.M. and Joo, J.J. "Variable camber compliant wing - Wind tunnel testing," *23rd AIAA/AHS Adaptive Structures Conference*, 2015, p 1051.
5. Joo, J.J., Marks, C.R., Zientarski, L. and Culler, A.J. "Variable camber compliant wing - Design," *23rd AIAA/AHS Adaptive Structures Conference*, Kissimmee, Florida, 2015 a, p 1050.

https://doi.org/10.1017/aer.2022.34 Published online by Cambridge University Press

6. Miller, S.C., Rumpfkeil, M.P. and Joo, J.J. "Fluid-structure interaction of a variable camber compliant wing," *53rd AIAA Aerospace Sciences Meeting*, Kissimmee, Florida, 2015, p 1235.
7. Joo, J.J., Marks, C.R. and Zientarski, L. "Active wing shape reconfiguration using a variable camber compliant wing system," *20th International Conference on Composite Materials*, Copenhagen, 2015 b, p 12.
8. Marks, C.R., Zientarski, L. and Joo, J.J. "Investigation into the effect of shape deviation on variable camber compliant wing performance," *24th AIAA/AHS Adaptive Structures Conference*, 2016, p 1313.
9. Kudva, J., Appa, K., Martin, C., Jardine, A., Sendeckyj, G., Harris, T., et al., "Design, fabrication, and testing of the DARPA/Wright lab 'Smart wing' wind tunnel model," *38th Structures, Structural Dynamics, and Materials Conference*, 1997, p 1198.
10. Hetrick, J., Osborn, R., Kota, S., Flick, P. and Paul, D. "Flight testing of mission adaptive compliant wing," *48th AIAA/ASME/ASCE/AHS/ASC Structures, Structural Dynamics, and Materials Conference*, 2007, p 1709.
11. Vos, R., Gurdal, Z. and Abdalla, M. "Mechanism for warp-controlled twist of a morphing wing," *J Aircr.*, 2010, **47**, (2), pp 450–457.
12. Kuchemann, D. "A simple method for calculating the span and chordwise loading on straight and swept wings of any given aspect ratio at subsonic speed." Tech. rep., Aeronautical Research Council London, 1956.
13. Boltz, F.W. and Kolbe, C.D. "The forces and pressure distribution at subsonic speeds on a cambered and twisted wing having 45 of sweepback, an aspect ratio of 3, and a taper ratio of 0.5," *NACA RMA52D22*, 1952.
14. Hall, I. and Rogers, E. "Experiments with a tapered sweptback wing of warren 12 planform at mach numbers between 0.6 and 1.6," RM-3271, *Aeronautical Research Council, London*, 1962.
15. Graham, R.R. "Low-speed characteristics of a 45 sweptback wing of aspect ratio 8 from pressure distributions and force tests at Reynolds numbers from 1,500,000 to 4,800,000," *NACA RM-L51H13*, 1951.
16. Weber, J. and Brebner, G. "Low speed tests on a 45-deg swept Back wings, Part-I: Pressure measurements on wings of aspect ratio 5," RM-2882, *Aeronautical Research Council, London*, 1958.
17. Phillips, W., Hunsaker, D.F. and Niewoehner, R. "Estimating the subsonic aerodynamic centre and moment components for swept wings," *J Aircr.*, 2008, **45**, (3) a, pp 1033–1043.
18. Magnus, A.E. and Epton, M.A. "PAN AIR: A computer program for predicting subsonic or supersonic linear potential flows about arbitrary configurations using a higher order panel method. Volume 1: Theory document (version 1.1)," 1981.
19. Hahn, M. and Drikakis, D. "Implicit large-eddy simulation of swept-wing flow using high-resolution methods," *AIAA J*, 2009, **47**, (3), pp 618–630.
20. Takeuchi, K., Matsushima, K., Kanazaki, M. and Kusunose, K. "CFD analysis on sweep angles of the leading and trailing edges of a wing in a supersonic flow," *Trans JSME (in Japanese)*, 2015, **81**, (827), pp 15–00037.
21. Thomas, J. and Miller, D. "Numerical comparisons of panel methods at subsonic and supersonic speeds," *17th Aerospace Sciences Meeting*, 1979, p 404.
22. Sytsma, H., Hewitt, B.L. and Rubbert, P. "A Comparison of panel methods for subsonic flow computation," Tech. Rep. AGARD-AG-241, Advisory Group for Aerospace Research and Development Neilly-sur-Seine, 1979.
23. Thomas, J., Luckring, J. and Sellers III, W. "Evaluation of factors determining the accuracy of linearized subsonic panel methods," *Applied Aerodynamics Conference*, 1983, p 1826.
24. Moorthamers, B. and Hunsaker, D.F. "Aerodynamic centre at the root of swept, elliptic wings in inviscid flow," *AIAA Scitech 2019 Forum*, American Institute of Aeronautics and Astronautics, San Diego, California, 2019.
25. Phillips, W., Alley, N. and Niewoehner, R. "Effects of nonlinearities on subsonic aerodynamic centre," *J Aircr.*, 2008, **45**, (4) b, pp 1244–1255.
26. Kuchemann, D. "The distribution of lift over the surface of swept wings," *Aeronaut Q*, 1953, IV, pp 437–444.
27. Torenbeek, E. *Advanced Aircraft Design: Conceptual Design, Analysis and Optimization of Subsonic Civil Airplanes*. John Wiley & Sons, 2013.

Cite this article: Moorthamers B. and Hunsaker D.F. (2022). Accuracy of Küchemann's prediction for the locus of aerodynamic centres on swept wings compared to an inviscid panel method. *The Aeronautical Journal*, **126**, 1853–1873. https://doi.org/10.1017/aer.2022.34

https://doi.org/10.1017/aer.2022.34 Published online by Cambridge University Press